Available online at www.sciencedirect.com
SCIENCE DIRECT®
Molecular & Biochemical Parasitology 128 (2003) 135–145
MOLECULAR & BIOCHEMICAL PARASITOLOGY

# Structural features affecting variant surface glycoprotein expression in *Trypanosoma brucei*

Jun Wang, Ulrike Böhme, George A.M. Cross*

*Laboratory of Molecular Parasitology, The Rockefeller University, Box 185, 1230 York Avenue, New York, NY 10021-6399, USA*

Received 6 December 2002; accepted 25 February 2003

**Abstract**

The glycosylphosphatidylinositol (GPI)-anchored variant surface glycoprotein (VSG) of *Trypanosoma brucei* is the most abundant GPI-anchored protein expressed on any cell, and is an essential virulence factor. To determine what structural features affect efficient expression of VSG, we made a series of mutations in two VSGs. Inserting 18 amino acids, between the amino- and carboxy-terminal domains, reduced the expression of VSG 221 to about 3% of the wild-type level. When this insertion was combined with deletion of the single carboxy-terminal subdomain, expression was reduced a further three-fold. In VSG 117, which contains two carboxy-terminal subdomains, point mutation of the intervening *N*-glycosylation site reduced expression about 15-fold. Deleting the most carboxy-terminal subdomain and intervening region, including the *N*-glycosylation site, reduced expression to 15–20% of wild type VSG, and deletion of both subdomains reduced expression to <1%. Despite their low abundance, all VSG mutants were GPI anchored on the cell surface. Our results suggest that, for a protein to be efficiently displayed on the surface of bloodstream-form *T. brucei*, it is essential that it contains the conserved structural motifs of a *T. brucei* VSG. Serum resistance-associated protein (SRA), which confers human infectivity on *T. brucei*, strongly resembles a VSG deletion mutant. Expression of three epitope-tagged versions of SRA in *T. brucei* conferred total resistance to human serum. SRA possesses a canonical GPI signal sequence, but we were unable to obtain unequivocal evidence for the presence of a GPI anchor. SRA was not released during osmotic lysis, indicating that it is not GPI anchored on the cell surface.


*Keywords:* Glycosylation; Human infectivity; Serum resistance-associated protein; *Trypanosoma brucei*; Variant surface glycoprotein; Virulence

## 1. Introduction

*Trypanosoma brucei* owes much of the credit for its survival, in the infected host, to its mechanism for antigenic variation, manifested in the sequential expression of genes encoding a large family of variant surface glycoproteins (VSGs). Each trypanosome expresses a single VSG, which accounts for about 10% of the total cellular protein. In most eukaryotic cells, however, GPI anchors are found on a minority of cell-surface proteins. Studies of *T. brucei* VSG structure provided the definitive chemical evidence, followed by the first complete structure [1], of a glycosylphosphatidylinositol (GPI) anchor moiety. The GPI anchor was subsequently found to be a universal feature of eukaryotic cells [2–5], although GPI-anchored surface proteins are particularly abundant in pathogenic protozoa [6].

Proteins that are destined to be GPI-anchored are translated with cleavable amino- and carboxy-terminal signal peptides. The amino-terminal signal peptide directs the nascent polypeptide to the endoplasmic reticulum, where the carboxy-terminal signal peptide is replaced by a preformed GPI anchor in an immediately posttranslational transamidation reaction catalyzed by a multi-protein complex. In all GPI-anchored proteins, the carboxy-terminal signal peptide has certain conserved features. It consists of a hydrophilic spacer sequence of 8–12 amino acids, followed by a more hydrophobic region of 8–20 amino acids. The site of GPI attachment is called the ω site [7]. Comparison of known and predicted GPI addition sites suggest that the ω site is restricted to six amino acids with small side chains, namely (in order of predominance) Ser > Asn > Asp > Gly, Ala and Cys, whereas ω + 2 can be Ala > Gly > Ser, Thr and Val. The ω + 1 position, where Ala > Ser > Asp > Thr, Arg, Cys, Met, Trp, is less restricted [5,8,9]. In comparison to

*Abbreviations:* IF, immunofluorescence; GPI, glycosylphosphatidylinositol; PIPLC, phosphatidylinositol phospholipase C, primarily the endogenous *T. brucei* enzyme that releases cell-surface GPI-anchored proteins; SRA, serum resistance associated; VSG, variant surface glycoprotein

* Corresponding author. Tel.: +1-212-327-7571; fax: +1-212-327-7845.
*E-mail address:* george.cross@rockefeller.edu (G.A.M. Cross).

0166-6851/03/$ – see front matter © 2003 Elsevier Science B.V. All rights reserved.
doi:10.1016/S0166-6851(03)00055-0

other GPI-anchored proteins, the VSG GPI signal sequence is remarkably conserved. The ω position is always Ser, Asp or Asn, and the length of the signal sequence is either 17 (ω Ser) or 23 (ω Asp) amino acids. Two positions in the spacer sequence are also remarkably conserved. ω + 2 is always Ser and ω + 7 is almost always Lys. We recently reported the effects of mutating the VSG GPI signal sequence on VSG expression and surface display [10]. Surprisingly, our results indicated that the high conservation of the VSG GPI signal sequence is unnecessary for efficient expression and GPI attachment, but addition of a GPI anchor is essential for surface expression of a VSG polypeptide.

*T. brucei* VSGs consist of two domains. The amino-terminal domain structures fall into two major classes, having either 4–6 or 10–12 cysteine residues. Carboxy-terminal subdomains contain four highly conserved cysteine residues and *T. brucei* VSGs contain either one or two subdomains. There is extensive variation in the amino acid sequence of the amino-terminal domain, but crystal structures of the amino-terminal domains of two VSGs, and structure-based alignment of other VSG sequences, suggest that the three-dimensional structure may be highly conserved [11]. The higher sequence conservation of the carboxy-terminal domains suggest that, although no structures have been determined, they will also be highly conserved.

In view of the unexpectedly minor or undetectable effects of interfering with conserved aspects of the VSG GPI signal sequence, and the previously reported difficulties in expressing non-VSG GPI-anchored proteins on the surface of *T. brucei* [10], we decided to investigate the effects of other variations of VSG structure on its expression and cell-surface GPI anchoring, since it appeared that, to be efficiently expressed, a protein has to look very much like a VSG and receive a GPI anchor. We also report some preliminary studies on a particularly relevant naturally occurring VSG mutant, encoded by the serum resistance-associated (*SRA*) gene, which transforms non-human-infective *T. brucei* into a virulent *T. brucei rhodesiense*-like human-infective species [12]. *SRA* is uniformly associated with current human isolates of that subspecies [13–15].

## 2. Materials and methods

### 2.1. Trypanosome culture and transfection

Bloodstream-form *T. brucei* Lister 427-derived cell lines were cultured in HMI-9 at 37 °C [16]. In case of toxicity, the various mutated VSGs were introduced with the pLew82 targeting vector, under tetracycline regulation in parental cells that express wild-type VSG 221 from the endogenous VSG expression site, together with T7 RNA polymerase and the tet repressor [17,18]. Expression of the selectable marker was induced by adding 2.5 ng ml$^{-1}$ doxycycline to the medium, after transfection. For maximum induction of mutant VSGs, doxycycline was added at 100 ng ml$^{-1}$ for 16–24 h. In fact, as is often the case with the pLew82 vector, the clones that we studied were not tightly regulated. We did not consider it necessary to screen many clones, to obtain ones that were tightly regulated, because none of the mutant proteins appeared to be toxic. *VSG 117* mutations were introduced into trypanosome cell line 13–90 and *VSG 221* and *SRA* constructs were expressed in the 'single marker' parental line [17,18]. All transfections were performed as described previously [19].

### 2.2. Generation of VSG mutations

The relevant structural features of all VSG and SRA constructs used in this work are summarized in Fig. 1. The various VSG constructs were made by PCR, ligation, and cloning from existing plasmids containing the relevant gene, introducing the mutations and insertions by appropriate use of synthetic oligonucleotides. All mutations were verified by standard sequencing techniques (Protein/DNA Technology Center, The Rockefeller University). Details are available on request.

### 2.3. Generation of HA-tagged SRA

HA-tagged SRA was generated by PCR. *SRA* (kindly provided by Luc Vanhamme) was subcloned into pLew82, creating SRA/pLew82 that was used as the template for two PCRs using forward primer (F5) 5′-CTCGAGATGCCCCGAAATTCGGG-3′ and reverse primer (R5) 5′-**TCTAGA**TTCTTTTCCTTCCCATTC-3′ or forward HA-tag primer (F6) 5′-**TCTAGA**ATGTACCCCTACGACGTTCCAGACTACGCATCCAAAGATTCAAGTTTTC-3′ and reverse primer R3. The two PCR fragments were ligated using the *Xb*1 restriction site that was introduced in the primers (in bold) to generate the carboxy-terminal HA-tagged SRA. To generate amino-terminal version1 HA-tagged SRA, the following primers were used: forward primer EW45 and reverse primer (R6) 5′-**TCTAGA**TGGTGCCAGCAGCTTTAGGGCCAG-3′ or forward HA-tag primer (F7) 5′-**TCTAGA**GGTACCGCTGTGTACCCCTACGACGTTCCAGACTACGCACCTGTATCGCCCAGTGGCACCGCCTTTGA-3′ and reverse primer R3. The two fragments were ligated using the *Xba*I site. To generate amino-terminal version2 HA-tagged SRA, the following primers were used: forward primer EW45 and reverse primer (R7) 5′-**TCTAGA**GTCAAAGGCGGTGCC-3′ or forward HA-tag primer (F8) 5′-**TCTAGA**TACCCCTACGACGTTCCAGACTACGCAGAAGAGCCCGTCAAGAAGGT-3′ and reverse primer R3. The two fragments were ligated using the *Xba*I site All three version of HA-tagged SRA were subcloned into pLew82. The sequences of all constructs were verified.

### 2.4. Western blot analysis

Samples corresponding to appropriate amounts of cells, based on preliminary measurements of expression levels,

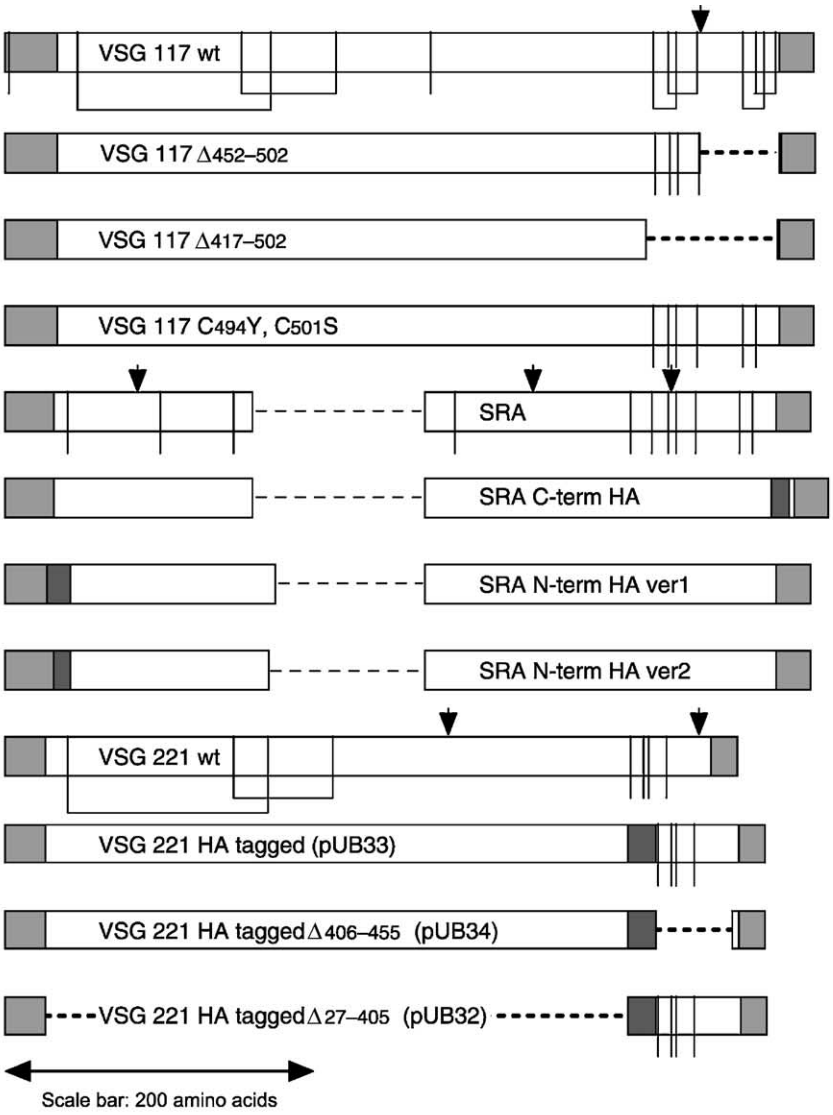


```
117 WT 411–526                ADQKGKSPESECNKISEEPKCNEDKICSWHKEVKAGEKHCKPNSTKAKEKGVSVTQTQTAGGTEATTDKCKGKLEDTCKKESNCKWENNACKDSSILVTKKFALTVVSAAFVALLF
117Δ452–502                   ADQKGKSPESECNKISEEPKCNEDKICSWHKEVKAGEKH                                                                CKDSSILVTKKFALTVVSAAFVALLF
117Δ417–502                   ADQKGK                                                                                                 VND SSILVTKKFALTVVSAAFVALLF

SRA WT 297–410          QVATNQAQEAFCNAIGDDKDKCNNETRCSYDDSKGSDKKCTYNAEKAEANGAPATQPQGGVNEATTGNCKGKLEPGCTKAQEYEWEGKE                SKDSSFLVDMKLALNMVAAFVAFLF
SRA HA insertion 386    QVATNQAQEAFCNAIGDDKDKCNNETRCSYDDSKGSDKKCTYNAEKAEANGAPATQPQGGVNEATTGNCKGKLEPGCTKAQEYEWEGKESRMYPYDVPDYASKDSSFLVDMKLALNMVAAFVAFLF

SRA WT 1–44             MPRNSGRTTSTLALAVALKLLAV                PVSPSGTAFD          EEPVKKVCKVE
SRA HA insertion ver1   MPRNSGRTTSTLALALALKLLAPSRGTAVYPYDVPDYAPVSPSGTAFD          EEPVKKVCKVE
SRA HA insertion ver2   MPRNSGRTTSTLALAVALKLLAV                PVSPSGTAFDSRYPYDVPDYAEEPVKKVCKVE

221 WT 401–476                                AETEG                SCNKKDQNECKSPCKWHNDAENKKCTLDKEEAKKVADETAKDGKTGNTNTTGSSNSFVISKTPLWLAVLLF
221 HA insertion 405 (pUB33)                  AETEGSRAYPYDVPDYASLGPGNSCNKKDQNECKSPCKWHNDAENKKCTLDKEEAKKVADETAKDGKTGNTNTTGSSNSFVISKTPLWLAVLLF
221 HA insertion 405/Δ406–455 (pUB34)         AETEGSRAYPYDVPDYASLGPGN                                                                TGS SNSFVISKTPLWLAVLLF
221 Δ27–405/HA insertion 405 (pUB32)                SRAYPYDVPDYASLGPGNSCNKKDQNECKSPCKWHNDAENKKCTLDKEEAKKVADETAKDGKTGNTNTTGSSNSFVISKTPLWLAVLLF
```

Fig. 1. Conserved features of *T. brucei* VSGs and SRA, showing deletions and point mutations created in VSGs 117 and 221, and the insertion positions of HA tags. VSG amino-terminal domains fall into two major classes, having either 4–6 or 10–12 cysteine residues. Carboxy-terminal subdomains contain four highly conserved cysteine residues and *T. brucei* VSGs contain either one or two subdomains. Either amino-terminal class can be paired with either carboxy-terminal motif. Disulfide linkages have been experimentally determined for VSG 117 [28] and VSG 221 [27] (indicated by the overlines connecting the vertical lines that indicate cysteine residues). Carboxy-domain cysteine residues are so highly conserved that they are likely to adopt the same pairing in other VSGs and in SRA. Cysteine residues are only indicated in mutant constructs where their positions are particularly relevant. Arrowheads indicate proven (VSG) or likely (SRA) *N*-glycosylation sites. Bold dashed lines indicate regions deleted in those VSG constructs and the light dashed line in SRA constructs represents a conceptual deletion, relative to VSGs. The mature amino-termini and the GPI attachment sites are known for VSGs 117 (D503) and 221 (S459), and predicted for SRA (D388). Cleaved signal sequences are indicated by light gray shading and insertions containing the HA epitope tag are shaded in a darker gray. The precise amino acid sequences of the insertions and surrounding wild-type sequences are shown in the lower part of the figure. Spaces have been inserted to allow conserved wild-type amino acids to remain aligned within each group of sequences. The nine amino acid HA tag is underlined. Sequences are from SwissProt, accession numbers P26332 (VSG 221), P02896 (VSG 117) and Z37159.1 (SRA): this is a corrected version (November 2002) of the originally reported sequence [55], which was kindly provided to us by Luc Vanhamme in 1999, and differs at four positions, including a G > C change, from a second published sequence (AF097331, [32]).

were run on 10 or 15% polyacrylamide-SDS gels and transferred onto nitrocellulose membranes (Amersham-Pharmacia). Tris-buffered saline, pH 7.6, plus 0.1% Tween-20 (TBST), containing 5% non-fat dry milk, was used as a blocking solution, for 1 h at room temperature. The membranes were subsequently incubated for 1 h either with mouse monoclonal 12CA5 or rat monoclonal 3F10 anti-HA antibodies (Roche Diagnostics Corporation), diluted 1:5000 or rabbit anti-native VSG 221 or anti-recombinant VSG 117 [20] (diluted 1:10,000), washed in TBST, then incubated with the corresponding horseradish peroxidase-conjugated goat-anti-mouse, anti-rat or anti-rabbit antibody (dilution 1:10 000) for 1 h. Proteins were visualized with the super-signal Pico chemiluminescence substrate (Pierce). As a standard to quantify the expression of HA-tagged VSG or SRA, we used different dilutions of known amounts of a 55 kDa HA-tagged JNK-2 protein (Santa Cruz Biotechnology).

### 2.5. PIPLC release assay for GPI anchoring

$1 \times 10^7$ cells were resuspended in 200 μl ice-cold water containing 0.1 mM TLCK and held on ice for 5 min. After centrifugation at $3000 \times g$ for 5 min, the supernatant was discarded. The cell ghosts were resuspended in 200 μl 10 mM sodium phosphate buffer, pH 8.0, containing 0.1 mM TLCK. After incubation at 37 °C for 15 min, the sample was centrifuged at $16{,}000 \times g$ for 15 min and the different steps of the protocol were analyzed by western blotting. This protocol quantitatively releases cell-surface GPI-anchored VSG, in the 37 °C incubation, by activating an endogenous phospholipase C that is GPI-specific under these conditions [21,22]. Most cytoplasmic proteins are released in the initial 0 °C lysis step [23]. In some experiments, the initial ice-cold water lysis step was omitted and cells were lysed for 15 min at 37 °C in 10 mM sodium phosphate buffer containing TLCK and PMSF. In all experiments a parallel blot was probed with anti-VSG 221 to confirm that the endogenous VSG 221, expressed by all transgenic cell lines, was being released under the conditions of the assay.

### 2.6. Human serum resistance assay

A minor variation on the classical serum-sensitivity test [24] was used. Trypanosomes at a concentration of $10^7$ ml$^{-1}$ in HMI-9 medium were mixed with an equal volume of human serum or HMI-9 medium and incubated for 20 min at room temperature. Two hundred microliter aliquots ($10^6$ trypanosomes) were injected intraperitoneally into groups of 3–5, 25–35 g CD-1 female mice. The parasitemia was monitored by tail snips from the third day onward. Trypanosomes that were resistant to human serum, and control untreated trypanosomes, caused a fatal parasitemia within 72–84 h. Serum-sensitive trypanosomes, monitored for up to 3 weeks, did not induce an infection except on one occasion in one mouse.

## 3. Results

### 3.1. Deletions in VSG 221 and their effects on expression level and GPI anchoring

The structures of all proteins used in this study are summarized in Fig. 1 and all results are summarized in Table 1. All mutant proteins were expressed in parental bloodstream-form *T. brucei* lines that constitutively expresses wild-type VSG 221. VSG 221 mutant proteins were distinguished by inserting the nine amino acid HA epitope tag into the mutated sequences. However, inserting just 18 amino acids, including the HA epitope, in what is thought to be a relatively unstructured ∼20 amino acid proteinase-accessible [25,26] 'hinge' region, between the end (position 386) of the N-terminal domain contained in the X-ray crystal structure [27] and the first Cys (position 407) of the single tightly folded carboxy-terminal domain [28], reduced expression to about 3% of the wild-type control (Fig. 2, UB33). To determine whether some domains and features are more important than others, for efficient VSG expression in bloodstream-form *T. brucei*, we made two deletions in the HA-tagged VSG 221 sequence (Fig. 1, constructs UB32 and UB34). Deletion of the carboxy-terminal domain reduced expression to about 1% of the wild-type level (Fig. 2, UB34). Deleting the amino-terminal domain (Fig. 2, UB32) reduced expression below 0.1% of the wild-type level. We do not have an explanation for the anomalous migration of UB32, compared to its predicted size (Table 1). It is possible that the GPI anchor is more highly glycosylated on the truncated protein. Expression levels (Table 1) were calculated by titration of cell-equivalents loaded per lane against a standard HA-tagged protein (data not shown, but see Fig. 5 for similar titration data on SRA), reacted with anti-HA antibody on the same blot. These estimates of protein levels, by comparative western blotting, are likely to have errors of 2–3-fold, especially at the lower expression levels. Nevertheless, the trend of mutating VSG sequences is very striking. Experi-

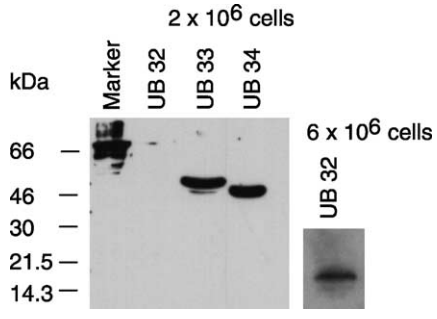


Fig. 2. Western blot comparing the different deletions of VSG 221. Cells were induced with 100 ng ml$^{-1}$ doxycycline for 24 h and the equivalent of $2 \times 10^6$ (large panel) or $6 \times 10^6$ (small panel) cells was loaded per lane on a 15% gel. The blot was exposed for 5 min (left panel) or 10 min (right panel). The marker lane contains the HA-tagged JNK protein.

Table 1
Properties of the sequences and mutations studied

| Source | Construct name | Mutation | Precursor length | Mature polypeptide | | Expression level (%)[a] | Surface GPI anchor |
|---|---|---|---|---|---|---|---|
| | | | | Length | Size (Da) | | |
| VSG 117 | | Wild type | 526 | 470 | 50217 | (100) | + |
| | | $N_{453}T$ | 526 | 470 | 50204 | 5–10 | + |
| | | $\Delta_{452-502}$ | 475 | 419 | 44707 | 15–20 | + |
| | | $\Delta_{417-502}$ | 442 | 386 | 40906 | <1 | + |
| | UB66 | $C_{494}Y$ & $C_{501}S$ | 526 | 470 | 50261 | ~100 | + |
| SRA | | Wild type | 410 | 357[b] | 37951 | ND | ND |
| | | N-terminal HA v1 | 425 | 375[b] | 39831 | 0.1–1.0 | – |
| | | N-terminal HA v2 | 421 | 368[b] | 39283 | 0.3–3.0 | – |
| | | C-terminal HA | 422 | 369[b] | 39414 | 1.0–10 | – |
| VSG 221 | | Wild type | 476 | 433 | 46291 | (100) | + |
| | UB33 | HA tag wild type | 494 | 451 | 48171 | ~3 | + |
| | UB34 | HA tag $\Delta_{406-455}$ | 444 | 401 | 42648 | ~1 | + |
| | UB32 | HA tag $\Delta_{27-406}$ | 115 | 71 | 7710 | <0.1 | – |

[a]Expression levels of SRA and VSG 221 mutants have been estimated relative to wild-type VSG 221 levels, by comparing intensities of HA-tagged SRA or VSG 221 bands with known amounts of a 55 kDa HA-tagged control protein loaded on the same gels, assuming $10^7$ molecules of wild-type VSG per cell. ND: not determined.

[b] Predicted mature SRA sizes are based on SignalP-predicted N-terminal signal sequence cleavage sites at position 28/29 for the N terminal HA version 1 and position 31/32 for the other three constructs, and assuming removal of a GPI signal sequence.

ments to determine whether the low steady-state levels of the mutant proteins were due to poor translation or rapid turnover of what the cell may detect as aberrant proteins, was beyond the scope of the current investigation.

Whether these VSG 221 deletions were cell-surface GPI anchored was determined by an osmotic lysis 'release assay', under conditions where an endogenous PIPLC cleaves surface-resident GPI-anchored VSG but not newly synthesized VSG that is within the secretory pathway [10,29,30]. The results (Fig. 3: compare the presence of protein in the 'S' versus 'P2' lanes) suggest that most of the detectable UB33 and UB34 proteins were cell-surface GPI anchored, but UB32 was not.

### 3.2. Effects of deletions and point mutations in VSG 117

N-linked glycans are important for protein folding and for monitoring the folded state, in the endoplasmic reticulum. Calreticulin is an important monitor of the folding process, by binding to mono-glucosylated high-mannose-type oligosaccharides. It is a conserved protein that was readily identifiable in fragmentary *T. brucei* genome data, and extracts of *T. brucei* contain a protein that reacts with antibodies to *Trypanosoma cruzi* calreticulin [31] (Jun Wang, unpublished data). We therefore investigated the effects of changing the single *N*-glycosylation site of VSG 117, at position 435, from asparagine to threonine ($N_{453}T$). The results (Fig. 4, panel A) show that the steady-state level was reduced to 5–10% of the level of wild-type VSG 117, expressed in the same VSG 221 parental cell line. The release assay (Fig. 4, panel B) indicated that the non-glycosylated protein was GPI anchored on the cell surface. Deletion of the most carboxy-terminal subdomain (including this glycosylation site), in such a way as to maintain the wild-type sequence immediately upstream of the GPI addition site (see lower panel in Fig. 1), reduced the steady state level to 15–20% of wild type and deletion of both subdomains reduced expres-

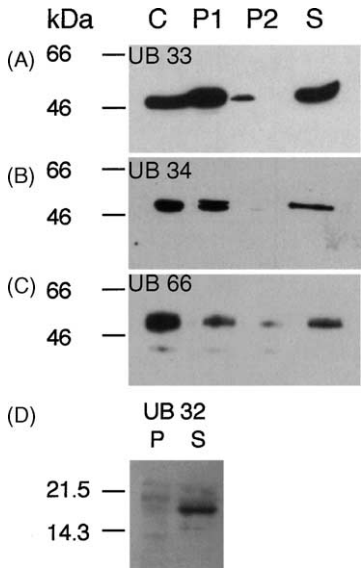


Fig. 3. Western blots after endogenous PIPLC activation to determine cell-surface GPI anchoring. Cells co-expressing the deletions and wild-type VSG 221 were osmotically lysed in ice-cold water (lane C). After centrifugation, the cell ghosts were resuspended (P1) then incubated in 10 mM sodium phosphate buffer, pH 8.0, at 37 °C for 15 min and centrifuged to generate pellet (P2) and supernatant (S) fractions. (A) UB33 (probed with mouse anti-HA). (B) UB34 (probed with mouse anti-HA). (C) UB66 (probed with rabbit anti-VSG 117). (D) UB32 (probed with rat anti-HA). The western blots A and B ($2 \times 10^6$ cell-equivalents in each lane) were exposed for 5 min, C ($2 \times 10^4$ cell-equivalents in each lane) for 10 s, and D ($6 \times 10^6$ cell-equivalents in each lane) for 10 min.

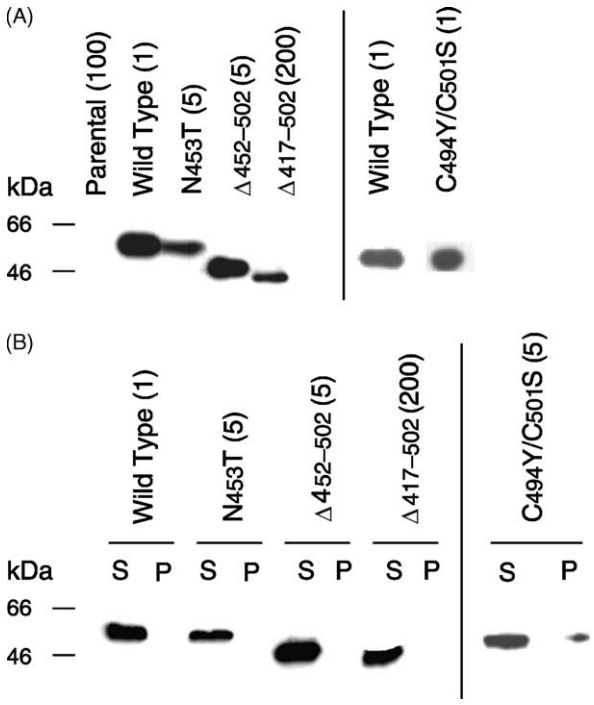


Fig. 4. Expression and cell-surface GPI anchoring of mutations in VSG 117. Western blots were probed with rabbit anti-VSG 117 antiserum. Numbers in parentheses represent the relative amounts of the different cell lines loaded on the gel, where 1 unit represents $2 \times 10^4$ (A) or $4 \times 10^4$ (B) cell-equivalents per lane. (A) Expression level, in whole cell extracts, of the non-glycosylated N453T mutant, carboxy-terminal sub domain deletions $\Delta_{452–502}$ and $\Delta_{417–502}$, and double cysteine mutant $C_{494}Y/C_{501}S$ (run on a separate gel at a different time). The parental cell line expresses VSG 221 but not 117. (B) PIPLC-release assay for GPI anchoring of the same mutants. S and P denote soluble (GPI anchored) and pellet (non-releasable) fractions.

sion to <1% (Fig. 4, panel A). What was detectable, for both of these constructs, was released after PIPLC activation.

For reasons that will be discussed in the next section, we mutated two cysteine residues (at positions 494 and 501) in the second carboxy-terminal subdomain, to destroy the two disulfide bonds that presumably stabilize the structure of the subdomain. in VSG 117. This double mutation, however, did not detectably affect expression level or GPI anchoring (Fig. 4), and these trypanosomes remained fully sensitive to human serum.

### *3.3. Expression of epitope-tagged SRA, a natural and important VSG deletion mutant*

Structural modeling of SRA, using the VSG amino-terminal X-ray structure (Mark Carrington, http://www.bio.cam.ac.uk/~mc115/: Andras Fiser and George Cross, unpublished data) strongly suggests that SRA is a VSG in which a contiguous stretch of the amino-terminal domain has been deleted. The carboxy-terminal domain is indistinguishable from that of a VSG, except for the absence of two cysteine residues, preventing formation of the two typical disulfide bonds. Because of the importance of SRA, we decided to perform similar experiments to those performed on the artificial VSG mutants, to investigate the expression, surface location and GPI anchoring of SRA. Because of the unavailability of SRA antibodies, we created versions of SRA in which an HA tag was inserted at three different and hopefully neutral positions. As we have shown here, insertion of the HA tag into the only internal site that we thought might not interfere with VSG expression (UB33) did, in fact, cause a 30-fold reduction in its expression level (Fig. 2 and Table 1), but did not affect its cell-surface GPI anchoring (Fig. 3). The only position in which an epitope tag has been added to a VSG without affecting its expression is immediately downstream of the amino-terminal signal sequence (Markus Engstler, personal communication). Because the mature SRA amino terminus is not known, and there could be some ambiguity in its prediction, we made two constructs in which the HA tag was inserted either three amino acids downstream of a 31 amino acid predicted signal peptide [32] (version 2: **MPRNSGRTTSTLALAVALKLLAVPVSPSGTA**FDsr ypydvpdyaEEPVKKVCK . . . ) or on a slightly longer extension that placed it three amino acids further upstream (version 1: **MPRNSGRTTSTLALALALKLLApsrgta**v ypydvpdyaPVSPSGTAFDEEPVKKVCK . . . ) and incorporated a predicted cleavage site upstream of the tag. In these sequences, the natural amino acids present in SRA are in upper case, the SignalP-predicted signal peptide is bold, the HA tag is underlined, and additional amino acids generated by the construction of the tagged versions are indicated in lower case. We also made a version in which the HA tag was inserted three amino acids upstream of the unambiguously predictable GPI attachment site (. . . WEGKESrmypydvpdyaSKD**SSFLVDMKLALNMVA** SKD**AFVAFLF**). To our knowledge, the effect of inserting this tag at the analogous position in a VSG has never been determined. When trypanosomes expressing any of the three HA-tagged SRA constructs were exposed to human serum, there was no reduction in their infectivity to mice, whereas the same number of the parental trypanosomes, treated in parallel, were not infective. Even at lower levels of expression from uninduced and mutated T7 promoters (pLew60 and pLew61 analogues [17] of the pLew82 expression vector), where SRA expression was undetectable on Western or Northern blots, SRA transgenic trypanosomes remained fully resistant to human serum, in the mouse-infectivity assay.

Fig. 5 illustrates the expression levels of the three SRA constructs, when fully induced by tetracycline. From the different gel loadings, in panels A and B, it is clear that the HA signal is about 10-fold higher in the carboxy-terminal HA-tagged construct than in the amino-terminal version 2, and the latter is about three-fold higher than the amino-terminal version 1. Northern blots showed about two-fold higher levels of steady-state RNA in cells expressing the carboxy-terminal HA-tagged SRA, in comparison

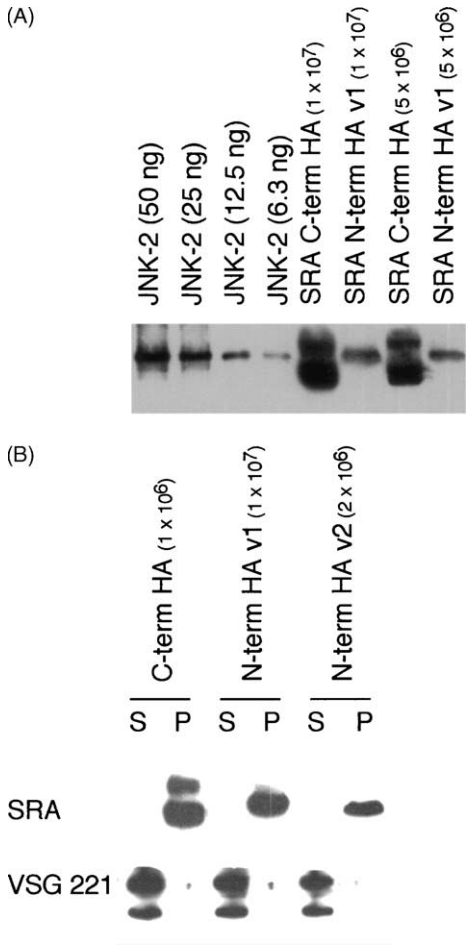


Fig. 5. SRA expression and cell-surface GPI anchoring. (A) Expression level of two HA-tagged SRA constructs determined by Western blot in comparison to a standard HA-tagged protein JNK-2, using rat anti-HA antibody 3F10. About two-thirds of the JNK-2 protein aggregated and remained close to the well of the gel. The amounts indicated, used for the estimation of SRA abundance, reflect the amount of the protein that migrates at the expected position (55 kDa, as shown) in the gel. Different numbers of cells were loaded, as indicated. Exposure time was 5 min. (B) SRA, detected with rat anti-HA antibody (top panel: exposed for 5 min), is not solublized after the one-step lysis and incubation, whereas a control using anti-VSG 221 antibody (lower panel: each lane contains $2 \times 10^5$ cell-equivalents and exposure time was 10 s) shows that the abundant VSG is released under the assay conditions.

with the N-terminal version 2 construct (data not shown). By using known amounts of a standard HA-tagged protein, JNK-2, we estimated that the expression level of the carboxy-terminal tagged SRA is from 1–10% of the level of VSG (Fig. 5, panel A). We could not estimate the expression level with greater accuracy, using the available reagents. We also have to consider the possibility, especially with amino-terminal tagged version 1, that not all of the protein is being processed at the predicted cleavage site. If alternative amino-terminal cleavages occurred, a fraction of the protein might loose the epitope tag.

In Fig. 5 (panel B), we show the results of a typical assay for the release of cell-surface GPI-anchored proteins, in all three SRA-expressing cell lines. No SRA was released in this assay, whereas the control blot shows that the endogenous VSG 221 was released. These results indicate the absence of detectable cell-surface GPI-anchored SRA in these cells. The presence of some SRA running higher than the predicted size might be due to different levels of glycosylation and is exaggerated in the more heavily expressing (overexposed) samples. The lower band in the overloaded VSG 221 blot is most likely a VSG degradation product.

This assay suggested that SRA might not receive a GPI anchor, or that it received a PIPLC-resistant anchor, in contrast to the VSG. In view of its highly conserved carboxy-terminal sequence, which is almost identical to that of VSG 117, it seemed highly unlikely that this would not be a functional GPI anchor signal. Similarly, it would be difficult to believe that the amino-terminal sequence would not act as an endoplasmic reticulum transit signal. Evidence that the amino-terminal signal is functional comes from the observation that SRA is *N*-glycosylated in these experiments, as evidenced by a small increase in SRA mobility when extracts were treated with endoglycosidase PNGaseF, for 2 h, in the presence of proteinase inhibitors (data not shown). We therefore labeled SRA-expressing cells with [$^3$H]-myristic acid, prepared extracts by detergent-solubilization in the presence of zinc, to inhibit the endogenous PIPLC, and immunoprecipitated both VSG and SRA, using VSG or HA antibodies (data not shown). However, due to the co-migration of SRA and VSG, we were unable to unequivocally prove that SRA was myristate labeled. Because of the lack of tetracycline regulation in the available clones, the obvious control of immunoprecipitating SRA from induced and uninduced cells could not be performed.

## 4. Discussion

In a previous paper [10], we reported that the highly conserved VSG GPI anchor signal sequence could be substantially modified without affecting GPI addition and VSG secretion. More drastic modifications that blocked GPI addition prevented the VSG from being displayed on the cell surface. We therefore concluded that GPI addition is essential for VSG to reach the cell surface. On the other hand, adding VSG signal sequences to alien GPI-anchored proteins, such as placental alkaline phosphatase, did not facilitate their appearance at the *T. brucei* cell surface (U. Böhme, Ph.D. Thesis, Universität Tübingen; Kelvin Davies, Markus Engstler, Ulrike Böhme and George Cross, unpublished data). This suggested that the folded VSG structure is also an important determinant of its efficient secretion. Although the amino acid sequences of *T. brucei* VSGs vary greatly, it has been proposed, based on the crystal structure of two VSG amino-terminal domains and structure-based alignment of others [11], that all VSGs have similar tertiary structures. In comparison to the amino-terminal domains, the amino acid sequence and disulfide bonds of the

carboxy-terminal subdomains are far more conserved between VSGs, so it seems likely that their folding is even more conserved, although this has not been experimentally verified. Interestingly, the seven VSGs of *T. congolense* [33–36] and one of *T. vivax* [37] that have been sequenced are much smaller than those of *T. brucei*, and they all lack the carboxy-terminal domain. The *T. vivax* VSG is also distinguished by not being *N*-glycosylated [37].

In view of these observations, we decided to investigate the effects, on expression and cell-surface GPI anchoring, of modifying other features of the VSG sequence. We made systematic small and large changes to the sequences of VSGs 117 and 221. The results of these experiments, on the mutant proteins schematized in Fig. 1, are summarized in Table 1. The most minor mutation that was introduced into VSG 221—the insertion of 18 amino acids, including the nine amino acid HA tag, into what we expected to be a rather neutral and unstructured region between the amino and carboxy-terminal domains—reduced the steady-state level to ∼3% of that of wild-type VSG 221. Combining the introduction of the HA tag with deletions in the VSG sequence was even more deleterious to VSG expression, although the products were GPI anchored. The VSG 117 mutations were more specific. When we mutated the single *N*-glycosylation site, expression was reduced about 15-fold, but the product was still GPI anchored. This shows that glycosylation is necessary for efficient expression, but not absolutely essential for some degree of expression. This is in line with current views on the role of glycosylation on the folding of secreted proteins. The main players in the endoplasmic reticulum folding pathway are BiP and calreticulin/calnexin, together with members of the protein disulfide isomerase family. The relative roles of BiP and calreticulin/calnexin may depend on the location of *N*-glycans in the polypeptide. If, as in the case of VSG 117, an *N*-glycan does not occur early in the linear sequence, the influence of calreticulin will be less important [38] and lack of glycosylation might not be expected to greatly affect folding, although other work suggests that calreticulin may still perform a chaperone function with non-glycosylated proteins [39]. *N*-Glycosylation can also play a role in the sorting of GPI-anchored proteins, on route to the cell surface [40].

Deletion of the second carboxy-terminal subdomain of VSG 117, including the single *N*-glycosylation site, reduced expression to about 20% of wild type VSG. Comparison of this deletion with the point mutation of the glycosylation site suggests that deletion of one carboxy-terminal domain would not, if a comparable glycosylation site had been retained, present a serious problem for VSG expression. Many VSGs—including VSG 221—contain only one subdomain, and a survey of VSG sequences suggests that amino and carboxy-terminal modules can be mixed and matched in any combination [41,42]. For VSG 117, deletion of both carboxy-terminal subdomains reduced expression to about 1%, although the product was still surface-GPI anchored. Thus, a mutant VSG that resembles a natural VSG from *T. vivax* or *T. congolense* is expressed at a very low level in *T. brucei*. At present, we can only speculate on whether the differences in virulence, between these trypanosome species, reflects differences in the expression efficiency of different VSG structures.

It should be noted that an expression level of 1% still represents 100,000 molecules per cell, which would be considered abundant for most cell-surface proteins. The GPI-anchored *T. brucei* transferrin receptor, which is also VSG-like in its structure [43], comprises less than 3000 molecules per cell [44] and two invariant transmembrane surface proteins, ISG65 and ISG75, are present at 70,000 and 50,000 molecules per cell, respectively [45,46]. It should be emphasized that the current experiments only measured the steady-state level of mutant VSGs and did not address the question of whether they were synthesized at a normal wild-type rate, then recognized as unnatural and eliminated by one of the degradative pathways that have been documented in other cell types. Such questions were not central to the aims of the present study. Previous studies, on the VSG GPI anchor signal sequence, showed that VSG mutants that were not correctly GPI anchored were unstable and rapidly degraded [10].

SRA, which confers human infectivity on *T. brucei* [12], strongly resembles a VSG deletion mutant. The SRA amino-terminal domain looks like that of a VSG, except for a deletion of about 100 contiguous amino acids, which is predicted to eliminate the surface loops of VSG but not to affect the VSG core structure (Mark Carrington, http://www.bio.cam.ac.uk/∼mc115/; Andras Fiser and George Cross, unpublished data). The carboxy-terminal domain structure is indistinguishable from that of a VSG, except that the second subdomain has two point mutations that would destroy the otherwise conserved disulfide bonds. Comparable mutations were introduced into VSG 117, to destroy the disulfide bonds of the second carboxy-terminal subdomain. Somewhat to our surprise, the expression of this mutant VSG was not detectably diminished (Table 1, construct UB66): nor were these cells resistant to human serum.

Because of the unavailability of antisera to wild-type SRA, we introduced an HA tag at three positions in the sequence. The only position in which an epitope tag has been added to a VSG without affecting its expression is immediately downstream of the amino-terminal signal sequence (Markus Engstler, personal communication). The mature amino terminus of SRA is not known. We therefore inserted an HA tag at two alternative positions that were predicted to leave the tag on the mature protein after cleavage of a signal sequence. An amino-terminal tag was perceived as having greater ultimate utility for future investigations of the subcellular location of SRA. In the third variant, we placed the tag immediately upstream of the mature carboxy terminus, which might be rather inaccessible if SRA were on the cell surface, based on early studies with antibodies to VSGs [47,48]. The HA signal varied over a 10-fold range, between the three tagged SRA cell lines (Table 1).

The strongest signal, which—in the first instance—would be presumed to indicate the highest expression level, was displayed by the carboxy-terminal tagged version. It is possible that variation in amino-terminal signal cleavage could compromise the relationship between SRA expression level and HA signal. Without antibodies to native SRA, or confirmation of the signal cleavage position, by sequencing mature purified HA-tagged SRA, we cannot definitively determine relative SRA expression levels.

We found that *T. brucei* expressing all three versions of SRA, even at low levels, rendered the cells resistant to human serum. Despite the presence of a canonical VSG GPI anchor signal sequence, none of the three tagged SRA were expressed as GPI-anchored cell-surface molecules, as indicated by the PIPLC release assay. Despite the equivocal results of myristic acid labeling, we think it is likely that SRA receives a GPI anchor. If so, there would be two possible explanations for the negative release results: either SRA contains a PIPLC-resistant GPI anchor, or it contains a normal anchor but is in a subcellular compartment where it is not accessible to PIPLC, during cell lysis. This is known to be the case for VSG in transit to the cell surface [29,30]. There are no precedents for different proteins receiving different GPI anchors in the same cell, but the GPI biosynthetic pathway, in bloodstream-form *T. brucei*, does produce both PIPLC-sensitive (lipid A) and PIPLC-insensitive (lipid C) versions of the final GPI molecule, which appear to be in equilibrium [49]. Only lipid A is transferred to VSG and the function of lipid C is unknown. There is one well characterized example of a GPI-anchored protein that might represent a precedent for SRA: the scrapie prion. PrPc is the normal cell-surface GPI-anchored version of the infectious prion form (PrPsc). PrPsc is essentially identical to PrPc in sequence, glycosylation, and in the structure of its GPI anchor [50,51], but PrPsc is highly proteinase resistant and differs in its tertiary structure. In contrast to PrPc, PrPsc cannot be labeled at the cell surface nor is it released by PIPLC treatment of cells [52]. Subsequent work suggests that PrPsc is sequestered within an endocytic compartment, and that conversion from cellular to scrapie form requires that the protein be GPI anchored and occurs either at the cell surface or in an early endocytic compartment [53]. This is an intriguing precedent for the possible pathway involved in SRA function.

An exhaustive study of SRA structure, location, and function, was beyond the intended scope of the present experiments. Nevertheless, our results provide a starting point for a broader study of SRA, and identify some of the issues that would have to be considered. Our results suggest that epitope tagging is a valid way of visualizing SRA. However, one would have to be cautious in investigating the subcellular location of SRA, in the quest to identify its mechanism of action, in a context where it is expressed well above the apparently very low level that is necessary to confer serum resistance [12], and the observable location of the detectable SRA may not reflect its true site of action. A major complication in imposing this rigorous standard, however, is that the minimal level of SRA expression that is necessary to cause human infectivity may be below the level of detection, by western blotting, radioisotopic labeling, or simple indirect immunofluorescence assays. More complex and sensitive microscopic techniques may be required. Nevertheless, its location under conditions of overexpression that are required to detect it might suggest avenues to pursue.

In conclusion, it appears that VSG structure, in *T. brucei*, has become highly optimized for efficient expression. This optimization might have been paralleled by evolution of specialized chaperone variants, or subtle optimization of the common chaperone pathways to favor efficient VSG expression, even to the disadvantage of other surface proteins. Nevertheless, such optimization could reflect another level for differential regulation of protein expression, in an organism that appears to largely bypass the possibility of regulating transcription initiation [54].

## Acknowledgements

This work was supported by the National Institutes of Health (grant number R03-AI43948), by the Deutsche Akademische Austauschdienst, and by private funds. We thank Jay Bangs, David Engman and Armondo Parodi for generous gifts of antibodies, Luc Vanhamme for the *SRA* plasmid and the corrected version of its sequence, Andras Fiser for modeling the SRA structure, and Markus Engstler, Peter Overath, Maarten Hoek and Simone Leal for helpful discussions.

## References

[1] Ferguson MAJ, Homans SW, Dwek RA, Rademacher TW. Glycosyl-phosphatidylinositol moiety that anchors *Trypanosoma brucei* variant surface glycoprotein to the membrane. Science 1988;239:753–9.
[2] Cross GAM. Glycolipid anchoring of plasma membrane proteins. Annu Rev Cell Biol 1990;6:1–39.
[3] Englund PT. The structure and biosynthesis of glycosyl phosphatidylinositol protein anchors. Annu Rev Biochem 1993;62:121–38.
[4] Udenfriend S, Kodukula K. How glycosylphosphatidylinositol-anchored membrane proteins are made. Annu Rev Biochem 1995;64:563–91.
[5] Udenfriend S, Kodukula K. Prediction of ω site in nascent precursor of glycosylphosphatidylinositol protein. Methods Enzymol 1995;250:571–82.
[6] Ferguson MAJ. The structure, biosynthesis and functions of glycosylphosphatidylinositol anchors, and the contributions of trypanosome research. J Cell Sci 1999;112:2799–809.
[7] Micanovic R, Gerber LD, Berger J, Kodukula K, Udenfriend S. Selectivity of the cleavage/attachment site of phosphatidylinositol-glycan-anchored membrane proteins determined by site-specific mutagenesis at Asp-484 of placental alkaline phosphatase. Proc Natl Acad Sci USA 1990;87:1–6.
[8] Bucht G, Hjalmarsson K. Residues in *Torpedo californica* acetylcholinesterase necessary for processing to a glycosyl phosphati-

dylinositol-anchored form. Biochim Biophys Acta 1996;1292:223–32.
[9] Bucht G, Wikstrom P, Hjalmarsson K. Optimising the signal peptide for glycosyl phosphatidylinositol modification of human acetylcholinesterase using mutational analysis and peptide-quantitative structure-activity relationships. Biochim Biophys Acta 1999;1431:471–82.
[10] Bohme U, Cross GAM. Mutational analysis of the variant surface glycoprotein GPI-anchor signal sequence in *Trypanosoma brucei*. J Cell Sci 2002;115:805–16.
[11] Blum ML, Down JA, Gurnett AM, Carrington M, Turner MJ, Wiley DC. A structural motif in the variant surface glycoproteins of *Trypanosoma brucei*. Nature 1993;362:603–9.
[12] van Xong H, Vanhamme L, Chamekh M, Chimfwembe CE, van den Abbeele J, Pays A, et al. A VSG expression-site-associated gene confers resistance to human serum in *Trypanosoma rhodesiense*. Cell 1998;95:839–46.
[13] Welburn SC, Picozzi K, Fevre EM, Coleman PG, Odiit M, Carrington M, et al. Identification of human-infective trypanosomes in animal reservoir of sleeping sickness in Uganda by means of serum-resistance-associated (SRA) gene. Lancet 2001;358:2017–9.
[14] Gibson W. Will the real *Trypanosoma brucei rhodesiense* please step forward? Trends Parasitol 2002;18:486–90.
[15] Gibson W, Backhouse T, Griffiths A. The human serum resistance associated gene is ubiquitous and conserved in *Trypanosoma brucei rhodesiense* throughout East Africa. Infect Genet Evol 2002;1:207–14.
[16] Hirumi H, Hirumi K. Continuous cultivation of *Trypanosoma brucei* bloodstream forms in a medium containing a low concentration of serum protein without feeder cell layers. J Parasitol 1989;75:985–9.
[17] Wirtz E, Hoek M, Cross GAM. Regulated processive transcription of chromatin by T7 RNA polymerase in *Trypanosoma brucei*. Nucleic Acids Res 1998;26:4626–34.
[18] Wirtz E, Leal S, Ochatt C, Cross GAM. A tightly regulated inducible expression system for dominant negative approaches in *Trypanosoma brucei*. Mol Biochem Parasitol 1999;99:89–101.
[19] Navarro M, Cross GAM. In situ analysis of a variant surface glycoprotein expression-site promoter region in *Trypanosoma brucei*. Mol Biochem Parasitol 1998;94:53–66.
[20] Hoek M, Xu H, Cross GAM. *Trypanosoma brucei*: generation of specific antisera to recombinant variant surface glycoproteins. Exp Parasitol 1999;91:199–202.
[21] Butikofer P, Boschung M, Brodbeck U, Menon AK. Phosphatidylinositol hydrolysis by *Trypanosoma brucei* glycosylphosphatidylinositol phospholipase C. J Biol Chem 1996;271:15533–41.
[22] Leal S, Acosta-Serrano A, Morita YS, Englund P, Bohme U, Cross GAM. Virulence of *Trypanosoma brucei* strain 427 is not affected by the absence of glycosylphosphatidylinositol phospholipase C. Mol Biochem Parasitol 2001;114:245–7.
[23] Cross GAM. Release and purification of *Trypanosoma brucei* variant surface glycoprotein. J Cell Biochem 1984;24:79–90.
[24] van Meirvenne N, Janssens PG, Magnus E. Further studies on the lytic and neutralizing action of human serum on *T. brucei*. Annales Soc Belge Med Trop 1973;53:49–56.
[25] Johnson JG, Cross GAM. Selective cleavage of variant surface glycoproteins from *Trypanosoma brucei*. Biochem J 1979;178:689–97.
[26] Ziegelbauer K, Stahl B, Karas M, Stierhof YD, Overath P. Proteolytic release of cell surface proteins during differentiation of *Trypanosoma brucei*. Biochemistry 1993;32:3737–42.
[27] Freymann D, Down J, Carrington M, Roditi I, Turner M, Wiley D. 2.9 Å resolution structure of the N-terminal domain of a variant surface glycoprotein from *Trypanosoma brucei*. J Mol Biol 1990;216:141–60.
[28] Allen G, Gurnett LP. Locations of the six disulphide bonds in a variant surface glycoprotein (VSG 117) from *Trypanosoma brucei*. Biochem J 1983;209:481–7.
[29] Bangs JD, Andrews NW, Hart GW, Englund PT. Posttranslational modification and intracellular transport of a trypanosome variant surface glycoprotein. J Cell Biol 1986;103:255–63.
[30] Ferguson MAJ, Duszenko M, Lamont GS, Overath P, Cross GAM. Biosynthesis of *Trypanosoma brucei* variant surface glycoproteins: *N*-glycosylation and addition of a phosphatidylinositol membrane anchor. J Biol Chem 1986;261:356–62.
[31] Labriola C, Cazzulo JJ, Parodi AJ. *Trypanosoma cruzi* calreticulin is a lectin that binds monoglucosylated oligosaccharides but not protein moieties of glycoproteins. Mol Biol Cell 1999;10:1381–94.
[32] Milner JD, Hajduk SL. Expression and localization of serum resistance associated protein in *Trypanosoma brucei rhodesiense*. Mol Biochem Parasitol 1999;104:271–83.
[33] Strickler JE, Binder DA, L'Italien JJ, Shimamoto GT, Wait SW, Dalheim LJ, et al. *Trypanosoma congolense*: structure and molecular organization of the surface glycoproteins of two early bloodstream variants. Biochemistry 1987;26:796–805.
[34] Rausch S, Shayan P, Salnikoff J, Reinwald E. Sequence determination of three variable surface glycoproteins from *Trypanosoma congolense*. Conserved sequence and structural motifs. Eur J Biochem 1994;223:813–21.
[35] Urakawa T, Eshita Y, Majiwa PAO. The primary structure of *Trypanosoma (nannomonas) congolense* variant surface glycoproteins. Exp Parasitol 1997;85:215–24.
[36] Bussler H, Linder M, Linder D, Reinwald E. Determination of the disulfide bonds within a B domain variant surface glycoprotein from *Trypanosoma congolense*. J Biol Chem 1998;273:32582–6.
[37] Gardiner PR, Nene V, Barry MM, Thatthi R, Burleigh B, Clarke MW. Characterization of a small variable surface glycoprotein from *Trypanosoma vivax*. Mol Biochem Parasitol 1996;82:1–11.
[38] Molinari M, Helenius A. Chaperone selection during glycoprotein translocation into the endoplasmic reticulum. Science 2000;288:331–3.
[39] Saito Y, Ihara Y, Leach MR, Cohen-Doyle MF, Williams DB. Calreticulin functions in vitro as a molecular chaperone for both glycosylated and non-glycosylated proteins. EMBO J 1999;18:6718–29.
[40] Benting JH, Rietveld AG, Simons K. *N*-Glycans mediate the apical sorting of a GPI-anchored, raft-associated protein in Madin-Darby canine kidney cells. J Cell Biol 1999;146:313–20.
[41] Carrington M, Miller N, Blum M, Roditi I, Wiley D, Turner MJ. Variant specific glycoprotein of *Trypanosoma brucei* consists of two domains each having an independently conserved pattern of cysteine residues. J Mol Biol 1991;221:823–35.
[42] Carrington M, Boothroyd J. Implications of conserved structural motifs in disparate trypanosome surface proteins. Mol Biochem Parasitol 1996;81:119–26.
[43] Salmon D, Hanocq-Quertier J, Paturiaux-Hanocq F, Pays A, Tebabi P, Nolan DP, Michel A, Pays E. Characterization of the ligand-binding site of the transferrin receptor in *Trypanosoma brucei* demonstrates a structural relationship with the N-terminal domain of the variant surface glycoprotein. EMBO J 1997;16:7272–8.
[44] Steverding D, Stierhof Y-D, Fuchs H, Tauber R, Overath P. Transferrin-binding protein complex is the receptor for transferrin uptake in *Trypanosoma brucei*. J Cell Biol 1995;131:1173–82.
[45] Ziegelbauer K, Multhaup G, Overath P. Molecular characterization of two invariant surface glycoproteins specific for the bloodstream stage of *Trypanosoma brucei*. J Biol Chem 1992;267:10797–803.
[46] Ziegelbauer K, Overath P. Organization of two invariant surface glycoproteins in the surface coat of *Trypanosoma brucei*. Infect Immun 1993;61:4540–5.
[47] Miller EN, Allan LM, Turner MJ. Topological analysis of antigenic determinants on a variant surface glycoprotein of *Trypanosoma brucei*. Mol Biochem Parasitol 1984;13:67–83.
[48] Masterson WJ, Taylor D, Turner MJ. Topologic analysis of the epitopes of a variant surface glycoprotein of *Trypanosoma brucei*. J Immunol 1988;140:3194–9.

[49] Guther MLS, Ferguson MAJ. The role of inositol acylation and inositol deacylation in GPI biosynthesis in *Trypanosoma brucei*. EMBO J 1995;14:3080–93.
[50] Stahl N, Baldwin MA, Hecker R, Pan KM, Burlingame AL, Prusiner SB. Glycosylinositol phospholipid anchors of the scrapie and cellular prion proteins contain sialic acid. Biochemistry 1992;31:5043–53.
[51] Rudd PM, Endo T, Colominas C, Groth D, Wheeler SF, Harvey DJ, et al. Glycosylation differences between the normal and pathogenic prion protein isoforms. Proc Natl Acad Sci USA 1999;96:13044–9.
[52] Stahl N, Borchelt DR, Prusiner SB. Differential release of cellular and scrapie prion proteins from cellular membranes by phosphatidylinositol-specific phospholipase C. Biochemistry 1990;29:5405–12.
[53] Vey M, Pilkuhn S, Wille H, Nixon R, Dearmond SJ, Smart EJ, et al. Subcellular colocalization of the cellular and scrapie prion proteins in caveolae-like membranous domains. Proc Natl Acad Sci USA 1996;93:14945–9.
[54] Clayton CE. Life without transcriptional control? From fly to man and back again. EMBO J 2002;21:1881–8.
[55] De Greef C, Hamers R. The serum resistance-associated (SRA) gene of *Trypanosoma brucei rhodesiense* encodes a variant surface glycoprotein-like protein. Mol Biochem Parasitol 1994;68:277–84.